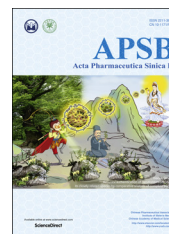




Chinese Pharmaceutical Association
Institute of Materia Medica, Chinese Academy of Medical Sciences

Acta Pharmaceutica Sinica B

www.elsevier.com/locate/apsb
www.sciencedirect.com



Cembrane-type diterpenoids from the South China Sea soft coral *Sarcophyton mililatensis*

Songwei Li^{a,b}, Fei Ye^a, Zhengdan Zhu^a, Hui Huang^c, Shuichun Mao^{b,*},
Yuewei Guo^{a,*}

^aState Key Laboratory of Drug Research, Shanghai Institute of Materia Medica, Chinese Academy of Sciences, Shanghai 201203, China

^bSchool of Pharmacy, Nanchang University, Nanchang 330006, China

^cKey Laboratory of Marine Bio-resources Sustainable Utilization, South China Sea Institute of Oceanology, Chinese Academy of Sciences, Guangzhou 510301, China

Received 26 March 2018; received in revised form 10 June 2018; accepted 12 June 2018

KEYWORDS

Soft coral;
Sarcophyton;
Sarcophyton mililatensis;
Cembrane-type diterpenoids;
Modified Mosher's method;
ECD calculation;
Cytotoxicity;
NF- κ B inhibitory activity

Abstract Eight cembrane-type diterpenoids, namely, (+)-(6*R*)-6-hydroxyisoscophytoxide (**1**), (+)-(6*R*)-6-acetoxyisoscophytoxide (**2**), (+)-17-hydroxyisoscophytoxide (**3**), sarcophilatins A–D (**4–7**), and sarcophilatol (**8**), were isolated from the soft coral *Sarcophyton mililatensis* collected from Weizhou Island, Guangxi Autonomous Region, together with 2 known related analogues, (+)-isoscophytoxide (**9**) and (+)-isoscophine (**10**). The structures of these compounds were elucidated by a combination of detailed spectroscopic analyses, chemical methods, and comparison with reported data. The absolute configuration of compound **1** was established by the modified Mosher's method, while the absolute configurations of compounds **4** and **5** were assigned by electronic circular dichroism (ECD) spectroscopy and that of compound **8** was established by time-dependent density functional theory electronic circular dichroism (TD-DFT ECD) calculation. In *in vitro* bioassays, compound **9** displayed significant cytotoxicity against the human cancer cell lines human promyelocytic leukemia cells (HL-60) and human lung adenocarcinoma cells (A-549) with IC₅₀ values of 0.78 ± 0.21 and 1.26 ± 0.80 μmol/L, respectively. Compounds **4** and **9** also showed moderate inhibitory effects on the TNF α -induced Nuclear factor kappa B (NF- κ B, a therapeutic target in cancer) activation, showing IC₅₀ values of 35.23 ± 12.42 and 22.52 ± 4.44 μmol/L, respectively.

© 2018 Chinese Pharmaceutical Association and Institute of Materia Medica, Chinese Academy of Medical Sciences. Production and hosting by Elsevier B.V. This is an open access article under the CC BY-NC-ND license (<http://creativecommons.org/licenses/by-nc-nd/4.0/>).

*Corresponding authors.

E-mail addresses: maoshuichun@ncu.edu.cn (Shuichun Mao), ywguo@sim.ac.cn (Yuewei Guo).

Peer review under responsibility of Institute of Materia Medica, Chinese Academy of Medical Sciences and Chinese Pharmaceutical Association

<https://doi.org/10.1016/j.apsb.2018.06.004>

2211-3835 © 2018 Chinese Pharmaceutical Association and Institute of Materia Medica, Chinese Academy of Medical Sciences. Production and hosting by Elsevier B.V. This is an open access article under the CC BY-NC-ND license (<http://creativecommons.org/licenses/by-nc-nd/4.0/>).

1. Introduction

Literature reports concerning the natural products chemistry of soft corals of the cosmopolitan genus *Sarcophyton* (Alcyonacea, Alcyoniidae) indicate that they are well-known to be a rich source of specialised metabolites, particularly diterpenoids of the cembrane-type^{1,2}. To date, more than 220 cembranes have been discovered, besides undefined species, from approximately 18 species of this genus. Moreover, some of them have been reported to be responsible for a diverse range of significant bioactivities, especially cytotoxic and anti-inflammatory effects²⁻⁴. Their excellent bioactivities have for a long time attracted great interest from synthetic organic chemists as challenging targets for total synthesis^{5,6}.

Sarcophyton species are prolific in the South China Sea. In the course of our ongoing search for bioactive secondary metabolites from the South China Sea marine invertebrates⁷⁻⁹, we collected the soft coral *S. mililatensis* from Weizhou Island, Guangxi Autonomous Region, China. Notably, only 2 prior phytochemical studies have been performed on this species collected from Bay Canh Island, Vietnam, resulting in the isolation of one 9,11-secosteroid and 6 cembranes^{10,11}. The present investigation of the Et₂O-soluble fraction from the acetone extract of *S. mililatensis* has now led to the discovery of eight previously undescribed cembrane-type diterpenoids, namely, (+)-(6*R*)-6-hydroxyisarcophytoxide (**1**), (+)-(6*R*)-6-acetoxyisarcophytoxide (**2**), (+)-17-hydroxyisarcophytoxide (**3**), sarcomililatin A–D (**4–7**), and sarcomililatol (**8**), along with 2 known structural analogues, (+)-isarcophytoxide (**9**) and (+)-isarcophine (**10**) as shown in Fig. 1. The absolute configuration of compound **1** was established by the modified Mosher's method. The absolute configurations of compounds **4** and **5** were assigned by ECD spectroscopy, while for compound **8** TD-DFT ECD calculation was used.

Cancer is a group of diseases characterized by uncontrolled cell growth, which has become the major public health concern over the last several decades¹²⁻¹⁵. NF- κ B, as a family of inducible transcription factors in all cells discovered by Sen and Baltimore¹⁶ in 1986, has become one of the major targets for drug development¹⁷. In particular, the aberrant activation of NF- κ B has been

frequently observed in various types of human cancers, and suppression of NF- κ B can limit the proliferation of cancer cells¹⁸. Hence, we focus on testing cytotoxic activity and the NF- κ B inhibitory effects. According to the results, compound **9** exhibited moderate cytotoxic activity, both compounds **4** and **9** showed moderate NF- κ B inhibitory effects on the TNF α -induced NF- κ B. Reported herein are the isolation and structural elucidation of these compounds as well as their biological properties.

2. Results and discussion

Compound **1** was isolated as a colorless oil, and had a molecular formula of C₂₀H₃₀O₃ as established by (+)-HR-ESI-MS ion peak at *m/z* 341.2096 [M + Na]⁺ (Calcd. for C₂₀H₃₀O₃Na, 341.2087) and ¹³C NMR data (Table 1), implying 6 degrees of unsaturation. Its IR spectrum showed the presence of a hydroxyl group (3363 cm⁻¹). The ¹H NMR spectrum (Table 1) displayed signals due to 3 vinyl methyls at δ_{H} 1.83 (3 H, s, H₃-19), 1.66 (3 H, s, H₃-17), and 1.60 (3 H, s, H₃-18), a tertiary methyl at δ_{H} 1.29 (3 H, s, H₃-20), and 2 olefinic protons appearing as doublets at δ_{H} 5.22 (1 H, d, *J* = 9.2 Hz, H-7) and 5.09 (1 H, d, *J* = 10.0 Hz, H-3), which were attributed to 2 trisubstituted double bonds. In addition, proton signals were also observed for one oxymethylene at δ_{H} 4.52 (1 H, dd, *J* = 12.0, 4.0 Hz, H-16a) and 4.47 (1 H, dd, *J* = 12.0, 3.2 Hz, H-16b) and 2 oxymethines at δ_{H} 5.38 (1 H, ddd, *J* = 10.0, 4.0, 3.2 Hz, H-2) and 2.39 (1 H, dd, *J* = 11.2, 2.8 Hz, H-11) in the ¹H NMR spectrum. The ¹³C NMR spectrum indicated the presence of 20 signals which were attributed by DEPT and HSQC experiments to 4 methyls, 6 methylenes, 5 methines, and 5 quaternary carbons. Of these carbons, 5 were bonded to oxygen and 6 were olefinic (2 were trisubstituted). These data suggested that **1** was a cembrane-type diterpenoid.

A comparison of the NMR data of **1** with those of the co-occurring known cembrane diterpenoid, (+)-isarcophytoxide (**9**)^{19,20}, revealed that they were structural analogues, with the only difference being the presence of an additional hydroxyl group at C-6 in **1**, in agreement with the mass data. The hydroxyl group

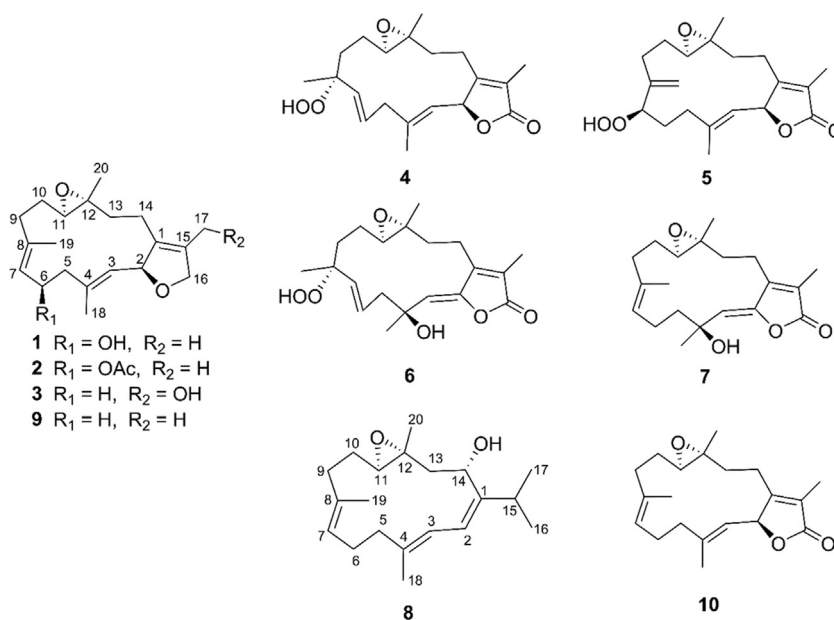


Figure 1 Chemical structures of compounds 1–10.

Table 1 ^1H NMR and ^{13}C NMR spectroscopic data for compounds **1–4** in CDCl_3^{a} .

Position	1 ^b		2 ^c		3 ^c		4 ^c	
	δ_{C} , type	δ_{H} (<i>J</i> in Hz)	δ_{C} , type	δ_{H} (<i>J</i> in Hz)	δ_{C} , type	δ_{H} (<i>J</i> in Hz)	δ_{C} , type	δ_{H} (<i>J</i> in Hz)
1	132.1, C		131.9, C		136.8, C		161.3, C	
2	83.0, CH	5.38, ddd (10.0, 4.0, 3.2)	82.9, CH	5.37, br d (10.2)	83.8, CH	5.45, ddd (10.2, 4.8, 3.6)	79.1, CH	5.42, d (10.2)
3	128.4, CH	5.09, d (10.0)	128.9, CH	5.11, d (10.2)	125.8, CH	5.09, d (10.2)	120.4, CH	4.91, d (10.2)
4	136.9, C		136.0, C		141.0, C		143.4, C	
5	48.4, CH ₂	2.16, dd (12.4, 10.8) 2.70, dd (12.4, 5.2)	44.9, CH ₂	2.22, dd (12.6, 10.8) 2.67, dd (12.6, 4.8)	39.0, CH ₂	2.18, m 2.31, m	42.1, CH ₂	2.80, dd (13.8, 7.2) 2.86, dd (13.8, 7.2)
6	65.4, CH	4.65, ddd (10.8, 9.2, 5.2)	67.9, CH	5.78, ddd (10.8, 10.2, 4.8)	22.8, CH ₂	1.09, m 2.42, m	129.6, CH	5.97, dt (15.6, 7.2)
7	128.5, CH	5.22, d (9.2)	124.3, CH	5.16, d (9.6)	125.7, CH	5.00, br d (9.0)	135.7, CH	5.62, d (15.6)
8	139.5, C		141.8, C		133.4, C		84.3, C	
9	36.8, CH ₂	2.02, m 2.35, m	36.6, CH ₂	2.01, m 2.36, m	36.8, CH ₂	1.97, m 2.29, m	35.4, CH ₂	1.81, m 1.85, m
10	23.7, CH ₂	1.28, m 2.13, m	23.7, CH ₂	1.28, m 2.15, m	24.3, CH ₂	1.25, m 1.69, m	24.0, CH ₂	1.66, m 1.76, m
11	62.1, CH	2.39, dd (11.2, 2.8)	61.8, CH	2.38, dd (10.2, 1.8)	62.5, CH	2.51, dd (10.8, 3.0)	61.7, CH	2.69, dd (7.8, 4.8)
12	61.7, C		61.5, C		61.5, C		61.0, C	
13	37.5, CH ₂	0.92, m 1.85, m	37.3, CH ₂	0.92, m 1.86, m	38.0, CH ₂	0.97, m 1.84, m	35.8, CH ₂	1.30, m 1.87, m
14	22.5, CH ₂	1.71, m 2.33, m	22.3, CH ₂	1.68, m 2.33, m	23.8, CH ₂	1.84, m 2.15, m	23.4, CH ₂	2.18, m 2.35, dt (13.2, 4.8)
15	128.8, C		128.7, C		132.0, C		123.8, C	
16	78.5, CH ₂	4.47, dd (12.0, 3.2) 4.52, dd (12.0, 4.0)	78.4, CH ₂	4.47, br d (11.4) 4.52, br d (11.4)	75.9, CH ₂	4.66, dd (12.0, 3.6) 4.76, dd (12.0, 4.8)	174.7, C	
17	10.1, CH ₃	1.66, s	10.0, CH ₃	1.66, s	57.0, CH ₂	4.26, d (12.6) 4.32, d (12.6)	9.1, CH ₃	1.85, br s
18	15.5, CH ₃	1.60, s	15.1, CH ₃	1.64, s	14.8, CH ₃	1.61, s	17.1, CH ₃	1.83, br s
19	14.9, CH ₃	1.83, s	15.3, CH ₃	1.83, s	14.9, CH ₃	1.66, s	21.2, CH ₃	1.47, s
20	15.8, CH ₃	1.29, s	15.7, CH ₃	1.29, s	15.9, CH ₃	1.28, s	16.7, CH ₃	1.30, s
6-OAc			170.2, C	2.03, s				
			21.4, CH ₃					
8-OOH								7.35, s

^a δ in ppm, assignments made by DEPT, COSY, HSQC, HMBC, and NOESY experiments.^bAt 400 MHz for ^1H and 100 MHz for ^{13}C NMR experiments.^cAt 600 MHz for ^1H and 150 MHz for ^{13}C NMR experiments.

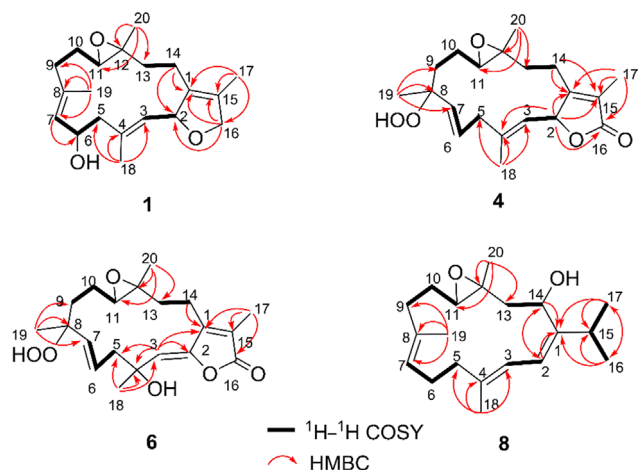


Figure 2 Selected ^1H - ^1H COSY and HMBC correlations of **1**, **4**, **6**, and **8**.

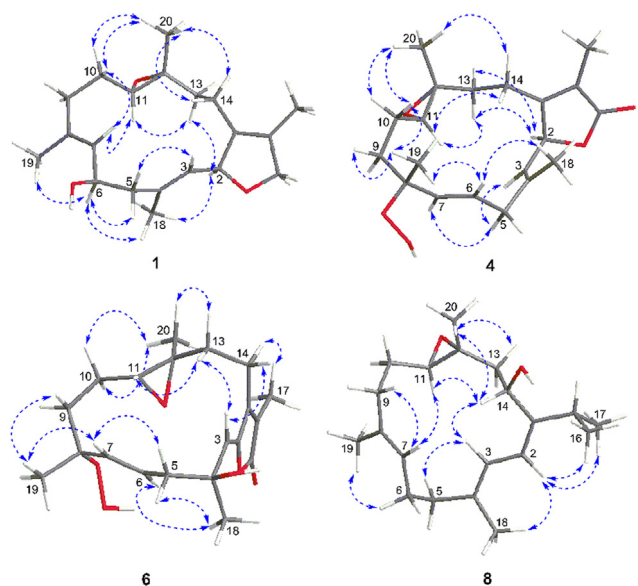


Figure 3 Key NOESY correlations for compounds **1**, **4**, **6**, and **8**.

was connected to C-6, as evidenced by the observation of the downfield chemical shift of C-6 from δ_{C} 24.5 to δ_{C} 65.4 in **1**. This assignment was further established by the ^1H - ^1H COSY cross-peaks (Fig. 2) of H-6 (δ_{H} 4.65) with both H₂-5 (δ_{H} 2.70 and 2.16) and H-7 (δ_{H} 5.22) and the HMBC correlation (Fig. 2) from H-7 to C-6. The geometries of the double bonds at Δ^3 and Δ^7 were assigned to be both *E* by the shielded carbon resonances of the 2 vinyl methyls at δ_{C} 15.5 (C-18) and 14.9 (C-19)²¹, which was further supported by the NOESY correlations (Fig. 3) of H₃-18 (δ_{H} 1.60)/H-2 (δ_{H} 5.38) and of H₃-19 (δ_{H} 1.83)/H-6 (δ_{H} 4.65). The relative configurations of C-2, C-11, and C-12 in **1** were proven to be the same as those of **9** due to the diagnostic NOESY correlations of H₃-20 (δ_{H} 1.29)/H₂-10 (δ_{H} 2.13 and 1.28) and H₂-14 (δ_{H} 2.33 and 1.71); H-11 (δ_{H} 2.39)/H-7 (δ_{H} 5.22) and H-13a (δ_{H} 0.92); and H-2/H-13a and H₃-18. Moreover, the NOESY correlations of H₃-18/H-6 and H-2 suggested that 6-OH was β -oriented.

The absolute configuration at C-6 of **1** was assigned *via* a modified Mosher's method. Esterification of **1** with (*R*)- and (*S*)-MTPA chloride occurred at the C-6 hydroxyl group to give the (*S*)- and (*R*)-MTPA ester derivatives, **1s** and **1r**, respectively. The observed $\Delta\delta_{\text{H}(S-R)}$ value distribution pattern (Fig. 4) established the 6*R*-configuration for **1**. Therefore, the structure of **1** was elucidated as (+)-(6*R*)-6-hydroxyisoscaphoxytoide.

Compound **2**, which was obtained as a colorless oil, gave the molecular formula $\text{C}_{22}\text{H}_{32}\text{O}_4$ on the basis of its (+)-HR-ESI-MS ion peak at m/z 383.2197 [$\text{M} + \text{Na}$]⁺ (Calcd. for $\text{C}_{22}\text{H}_{32}\text{O}_4\text{Na}$, 383.2193), requiring 7 degrees of unsaturation. The IR spectrum displayed a strong absorption at 1732 cm^{-1} , consistent with the presence of a saturated ester carbonyl group. The ^1H and ^{13}C NMR spectra (Table 1) of **2** were virtually identical to those of **1**, with the exception of an acetoxy moiety in **2** instead of the C-6 hydroxyl group in **1**. This replacement caused the ^{13}C NMR resonance of C-6 to be shifted downfield (from δ_{C} 65.4 to δ_{C} 67.9). The position of the acetoxy group at C-6 was further secured by the HMBC correlation (Fig. 2) from H-6 (δ_{H} 5.78) and the ester carbonyl carbon (δ_{C} 170.2). The similar NOESY correlation (Fig. 3) patterns of **2** and **1** indicated that they have the same relative configuration. Finally, the absolute configuration of **2** was assigned as 2*S*,6*R*,11*R*,12*R*, the same as those of **1**. This is because acetylation of **1** yielded **2**, which gave optical rotations $\{[\alpha]_{\text{D}}^{25} +51$ (*c* 0.09, CH_3OH); $[\alpha]_{\text{D}}^{25} +65$ (*c* 0.09, CHCl_3)\}, compared to those $\{[\alpha]_{\text{D}}^{25} +53$ (*c* 0.5, CH_3OH); $[\alpha]_{\text{D}}^{25} +63$ (*c* 0.24, CHCl_3)\} observed for the natural sample of **2**. The structure of **2** was thereby proposed as (+)-(6*R*)-6-acetoxyisoscaphoxytoide.

A literature search revealed that the assigned structure of **2** was the same as that of sarcophytonoxide A, a known cembrane diterpenoid isolated previously from the soft coral *Sarcophyton ehrenbergi*²². Furthermore, the ^1H and ^{13}C NMR data of **2** were also the same as those of sarcophytonoxide A. However, when the optical rotation of **2** (dextrorotatory, $[\alpha]_{\text{D}}^{25} +53$ (*c* 0.5, CH_3OH)), recorded in the same conditions, was compared with that reported for sarcophytonoxide A (levorotatory, $[\alpha]_{\text{D}}^{25} -36.8$ (*c* 0.5, CH_3OH))²², it appeared quite equal in value but opposite in sign. This result indicated that the 2 compounds are enantiomers and that the absolute configuration of sarcophytonoxide A should be 2*R*,6*S*,11*S*,12*S*.

Compound **3** was isolated as a colorless oil. Its molecular formula of $\text{C}_{20}\text{H}_{30}\text{O}_3$, the same as that of **1**, was deduced from the (+)-HR-ESI-MS ion peak at m/z 341.2077 [$\text{M} + \text{Na}$]⁺ (Calcd. for $\text{C}_{20}\text{H}_{30}\text{O}_3\text{Na}$, 341.2087). A comparison of the ^1H and ^{13}C NMR data (Table 1) of **3** and **1** indicated similarities between them. In fact, the structure of **3** differed from that of **1** only by the location of the hydroxyl group from C-6 to C-17 in **3**. This deduction was based on the chemical shift observed for C-6 (δ_{C} 22.8) and C-17 (δ_{C} 57.0), which was further confirmed by the ^1H - ^1H COSY cross-peaks (Fig. 2) of H₂-5 (δ_{H} 2.31 and 2.18)/H₂-6 (δ_{H} 2.42 and 1.09)/H-7 (δ_{H} 5.00) and the HMBC correlations (Fig. 2) from H₂-17 to C-1 (δ_{C} 136.8), C-15 (δ_{C} 132.0), and C-16 (δ_{C} 75.9). The relative configurations of all the asymmetric centers were determined to be the same as those of **1** on the basis of the NOESY experiment (Fig. 3). According to the previous findings^{2,19}, the absolute configuration at C-2 of **3** was proposed as *S* from the large dextrorotatory optical rotation $\{[\alpha]_{\text{D}}^{25} +98$ (*c* 0.1, CHCl_3)\}. The absolute configuration of **3** was tentatively assigned as 2*S*,11*R*,12*R*. Hence, the structure of **3** was shown to be (+)-17-hydroxyisoscaphoxytoide.

Compound **4** was obtained as a colorless oil with the molecular formula of $\text{C}_{20}\text{H}_{28}\text{O}_5$ on the basis of (+)-HR-ESI-MS ion peak at m/z 371.1822 [$\text{M} + \text{Na}$]⁺ (Calcd. for $\text{C}_{20}\text{H}_{28}\text{O}_5\text{Na}$, 371.1829) and ^{13}C NMR data (Table 1), suggesting that **4** possessed 7 degrees of

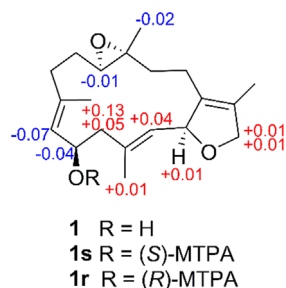


Figure 4 $\Delta\delta_{\text{H}}$ values [$\Delta\delta$ (in ppm) = $\delta_{\text{S}} - \delta_{\text{R}}$] obtained for (S)- and (R)-MTPA esters of compound **1** in pyridine- d_5 .

unsaturation. Its IR spectrum exhibited a broad absorption at 3356 cm^{-1} (OH) and strong absorptions at 1751 and 1678 cm^{-1} , consistent with the presence of an α,β -unsaturated γ -lactone moiety. This was supported by the ^{13}C NMR signals at δ_{C} 174.7 (C-16), 161.3 (C-1), 123.8 (C-15), and 79.1 (C-2) and UV absorption maxima at 246 and 275 nm²³. The third oxygen atom was determined to be part of a trisubstituted epoxy ring, which was confirmed by the appearance of signals at δ_{H} 2.69 (1 H, dd, $J = 7.8, 4.8$ Hz, H-11) and δ_{C} 61.7 (C-11) and 61.0 (C-12). The NMR signals of an oxygenated quaternary carbon and an exchangeable proton were observed at δ_{C} 84.3 (C-8) and δ_{H} 7.35 (1 H, s, 8-OOH), respectively, strongly implying that the remaining 2 oxygen atoms were involved in a hydroperoxy group²⁴. This conclusion was also supported by the significant downfield shift of the resonance for C-8 in **4** with respect to that of the corresponding carbon (δ_{C} 72.6) for mayolide B, a known cembranoid with the same 14-membered ring substituted with a hydroxy group at C-8 previously isolated the soft coral *Simularia mayi*²⁵. Further analysis of the ^{13}C NMR and DEPT spectra of **4** displayed 20 signals for 4 methyls, 5 methylenes, 5 methines (3 olefinic and 2 oxygenated), 5 quaternary carbons (3 olefinic and 2 oxygenated), and one conjugated ester carbonyl carbon (C-16). The planar structure of **4** was extensively elucidated by ^1H - ^1H COSY and HMBC spectra (Fig. 2). The ^1H - ^1H COSY cross-peaks readily determined the presence of 4 spin systems from H-2 to H-3; H₂-5 to H-7; H₂-9 to H-11; and H₂-13 to H₂-14. The significant HMBC correlations from Me-17 to C-1, C-15, and C-16; Me-18 to C-3, C-4, and C-5; Me-19 to C-7, C-8, and C-9; Me-20 to C-11, C-12, and C-13; H-2 to C-1, C-15, and C-16; and H₂-14 to C-1 and C-15 constructed the cembrane skeleton as depicted in Fig. 1. The hydroperoxy group and the epoxy ring in **4** were placed at C-8 and C-11/C-12, respectively, based on the strong HMBC correlations from Me-19 to C-8 and from Me-20 to C-11 and C-12.

The relative configuration of **4** was deduced from interpretation of the coupling constants and a NOESY experiment (Fig. 3). The large coupling constants ($J_{6,7} = 15.6$ Hz) and the chemical shift of the C-18 methyl group (δ_{C} 17.1) established the *E* geometries of the Δ^3 and Δ^6 double bonds, and this was further supported by the strong NOESY cross-peaks of H-6 (δ_{H} 5.97)/Me-18 (δ_{H} 1.83) and Me-19 (δ_{H} 1.47) and of H-5a (δ_{H} 2.86)/H-3 (δ_{H} 4.91) and H-7 (δ_{H} 5.62). The observed correlations in the NOESY spectrum as shown in Fig. 3 assigned H-11, Me-19, and Me-20 as β -oriented, while H-2 was the α -orientation. Furthermore, the absolute configuration at C-2 in **4** was defined by an ECD experiment. The ECD spectrum of **4** (Fig. 5) showed a negative Cotton effect at 249 nm ($\Delta\epsilon = -3.1$) and a positive Cotton effect at 221 nm ($\Delta\epsilon = +33.4$), indicative of a 2S-configuration^{26–28}. Accordingly, the structure of **4** was

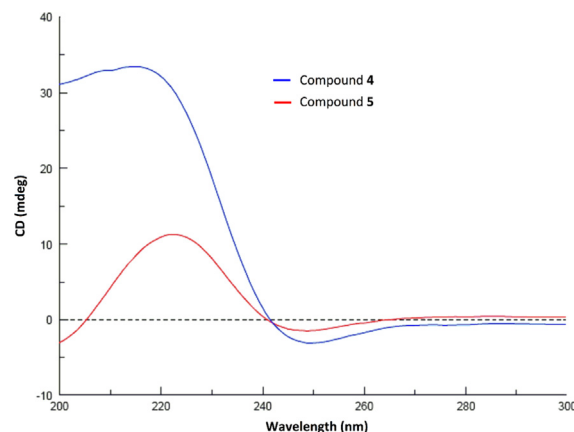


Figure 5 ECD spectra for compounds **4** (0.0014 mol/L, CH_3CN , cell length 2 cm) and **5** (0.0014 mol/L, CH_3CN , cell length 2 cm).

characterized as shown, and the compound was designated with the trivial name sarcomilatin A.

Compound **5** was isolated as a colorless oil, possessing the same molecular formula of $\text{C}_{20}\text{H}_{28}\text{O}_5$ as **4** by (+)-HR-ESI-MS ion peak at m/z 371.1830 [$\text{M} + \text{Na}$]⁺ (Calcd. for $\text{C}_{20}\text{H}_{28}\text{O}_5\text{Na}$, 371.1829). The IR, UV, and 1D NMR data (Table 2) of **5** were similar to those of **4**, except for the migration of the Δ^6 double bonds in **4** to $\Delta^{8(19)}$ [δ_{H} 5.24 (1 H, br s, H-19a) and 5.18 (1 H, br s, H-19b); δ_{C} 148.4 (s, C-8) and 113.8 (t, C-19)] and the position of the hydroperoxy group at C-8 in **4** to C-7 [δ_{H} 7.71 (1 H, s, 7-OOH) and 4.22 (1 H, dd, $J = 7.6, 5.6$ Hz, H-7); δ_{C} 83.3 (d, C-7)]. However, a literature survey revealed that **5** showed exactly the same ^1H and ^{13}C NMR data as trocheliolide A, a known cembrane diterpenoid isolated previously from the soft coral *Sarcophyton trocheliophorum*²⁹. This observation readily prompted us to assign the structure of **5** as trocheliolide A. Nevertheless, the optical rotations {dextrorotatory, $[\alpha]_{\text{D}}^{25} +34$ (c 0.1, CHCl_3) and $[\alpha]_{\text{D}}^{25} +23$ (c 0.1, CH_3OH)} sign of **5** as opposite to that of trocheliolide A {levorotatory, $[\alpha]_{\text{D}}^{26} -76$ (c 0.3, CHCl_3)}²⁹. These results suggested that **5** is the enantiomer of trocheliolide A. Moreover, the absolute configuration at C-2 in **5** was deduced to the same (S) as in **4** on the basis of an ECD spectrum with ϵ values (-1.5 at 249 nm and $+11.3$ at 223 nm). Thus, the structure of **5** (the trivial name sarcomilatin B) was assigned as depicted.

Compound **6** was obtained as a colorless oil. The molecular formula of **6** was established as $\text{C}_{20}\text{H}_{28}\text{O}_6$ based on the $[\text{M} - \text{H}]^-$ ion peak at m/z 363.1813 (Calcd. for $\text{C}_{20}\text{H}_{27}\text{O}_6$, 363.1813) in its (–)-HR-ESI-MS, which was 16 mass units more than that of **4**, appropriate for 7 degrees of unsaturation. The IR spectrum of **6** closely resembled that of **4**, showing similar functionalities in the molecule. Analysis of the ^1H and ^{13}C NMR spectra (Table 2) of **6** also revealed similarities to **4**, except for the location of one of the double bond from the Δ^3 to Δ^2 accompanied by hydroxylation occurring at C-3 in **6**. These observations were supported by the HMBC correlations (Fig. 2) from the olefinic proton H-3 resonating at δ_{H} 5.31 to C-1 (δ_{C} 151.0), C-2 (δ_{C} 147.8), C-4 (δ_{C} 73.7), C-5 (δ_{C} 47.0), and C-18 (δ_{C} 29.6) and from the methyl proton singlet H₃-18 (δ_{H} 1.55) to C-3 (δ_{C} 115.6), C-4, and C-5. Its relative configurations at C-8, C-11, and C-12 were proven the same as those of **4** on the basis of a NOESY experiment (Fig. 3). The diagnostic NOESY cross-peaks of H₃-19/H-7 and of H₃-18/one of the H₂-5 protons (δ_{H} 2.53) and H-6 (δ_{H} 5.81) suggested that Me-18 was α -oriented. Finally, from a biogenetic point of view, the

Table 2 ^1H and ^{13}C NMR spectroscopic data for compounds **5–8** in CDCl_3^{a} .

Position	5^c		6^b		7^c		8^b	
	δ_{C} , type	δ_{H} (<i>J</i> in Hz)	δ_{C} , type	δ_{H} (<i>J</i> in Hz)	δ_{C} , type	δ_{H} (<i>J</i> in Hz)	δ_{C} , type	δ_{H} (<i>J</i> in Hz)
1	161.2, C		151.0, C		151.3, C		149.0, C	
2	78.9, CH	5.49, dd (10.0, 1.6)	147.8, C		147.4, C		119.0, CH	6.02, d (10.8)
3	122.5, CH	5.05, dt (10.0, 1.2)	115.6, CH	5.31, s	116.4, CH	5.50, s	119.0, CH	5.93, d (10.8)
4	142.8, C		73.7, C		72.9, C		137.7, C	
5	35.8, CH ₂	2.22, m 2.47, ddd (13.2, 9.6, 6.8)	47.0, CH ₂	2.53, m	42.7, CH ₂	1.82, ddd (13.6, 9.6, 2.4) 1.97, ddd (13.6, 5.2, 2.0)	38.1, CH ₂	2.20, m
6	27.5, CH ₂	1.81, m	126.8, CH	5.81, dt (15.6, 7.2)	23.2, CH ₂	2.22, m 2.41, m	25.0, CH ₂	2.21, m 2.30, m
7	83.3, CH	4.22, dd (7.6, 5.6)	136.1, CH	5.63, d (15.6)	127.4, CH	5.26, t (6.8)	127.3, CH	5.15, dd (6.0, 4.2)
8	148.4, C		84.3, C		134.0, C		133.3, C	
9	31.5, CH ₂	2.22, m 2.35, m	35.0, CH ₂	1.50, m 1.97, m	36.5, CH ₂	2.07, m 2.26, m	36.9, CH ₂	1.09, m 2.24, m
10	30.3, CH ₂	1.54, m 2.08, m	22.7, CH ₂	1.45, m 1.73, m	24.6, CH ₂	1.53, m 1.85, m	24.5, CH ₂	1.70, m 1.78, m
11	62.9, CH	2.61, dd (10.0, 2.8)	62.5, CH	2.70, dd (7.2, 4.8)	60.6, CH	2.71, dd (7.2, 5.2)	62.4, CH	2.68, dd (7.2, 3.0)
12	61.2, C		60.3, C		60.4, C		61.6, C	
13	35.3, CH ₂	1.35, td (13.2, 4.0) 2.03, m	35.9, CH ₂	1.60, m 2.19, m	35.3, CH ₂	1.64, m 2.17, ddd (14.4, 8.4, 6.8)	46.0, CH ₂	1.28, dd (14.4, 1.8) 2.31, dd (14.4, 7.8)
14	22.8, CH ₂	2.26, m 2.38, m	20.1, CH ₂	2.40, ddd (15.0, 10.2, 4.8) 2.55, m	19.8, CH ₂	2.28, m 2.42, m	69.4, CH	4.86, dd (7.8, 1.8)
15	124.0, C		124.4, C		123.8, C		27.6, CH	2.55, septet (6.6)
16	174.7, C		169.7, C		169.7, C		24.5, CH ₃	1.07, d (6.6)
17	9.1, CH ₃	1.85, dd (1.6, 1.2)	9.4, CH ₃	1.93, s	9.3, CH ₃	1.94, s	25.2, CH ₃	1.09, d (6.6)
18	16.0, CH ₃	1.84, br s	29.6, CH ₃	1.55, s	30.1, CH ₃	1.41, s	17.6, CH ₃	1.71, br s
19	113.8, CH ₂	5.18, br s 5.24, br s	23.2, CH ₃	1.43, s	15.5, CH ₃	1.66, br s	15.3, CH ₃	1.65, br s
20	17.0, CH ₃	1.29, s	17.4, CH ₃	1.24, s	17.6, CH ₃	1.30, s	18.2, CH ₃	1.40, s
7-OOH		7.71, s						
8-OOH				7.40, s				

^a δ in ppm, assignments made by DEPT, COSY, HSQC, HMBC, and NOESY experiments.^bAt 600 MHz for ^1H and 150 MHz for ^{13}C NMR experiments.^cAt 400 MHz for ^1H and 100 MHz for ^{13}C NMR experiments.

absolute configurations at C-8, C-11, and C-12 of **6** were suggested to be the same as those of **4**. The absolute configuration of **6** was tentatively defined as 4*S*,8*R*,11*R*,12*R*. Accordingly, the structure of **6** (the trivial name sarcomililatin C) was characterized as depicted.

Compound **7** was isolated as a colorless oil. The HR-ESI-MS of **7** showed a fragment ion peak at m/z 315.1957 $[M - H_2O + H]^+$ (Calcd. for $C_{20}H_{27}O_3$, 315.1955) corresponding to the loss of water from **7**, suggesting a molecular formula of $C_{20}H_{28}O_4$ with 7 degrees of unsaturation. The 1H and ^{13}C NMR spectra (Table 2) of **7** showed similarities to those of **6**. However, the signal resonating at δ_H 7.40 (1 H, s) for the hydroperoxy group at C-8 in **6** was absent. Also, the 2 mutually coupled olefinic proton signals at δ_H 5.81 (1 H, dt, $J = 15.6, 7.2$ Hz, H-6) and 5.63 (1 H, d, $J = 15.6$ Hz, H-7) in **6** were replaced by an olefinic proton triplet at δ_H 5.26 (1 H, t, $J = 6.8$ Hz, H-7) in **7**. The above observations, combined with the 1H - 1H COSY cross-peaks (Fig. 2) of H₂-6 (δ_H 2.41 and 2.22) with H-7 and the HMBC correlations from H₃-19 (δ_H 1.66) to C-7 (δ_C 127.4) and C-8 (δ_C 134.0), indicated the loss of the hydroperoxy group in **6** accompanied by the isomerization of the olefin from the Δ^6 to Δ^7 . The *E* geometry of the Δ^7 double bond in **7** was suggested by the chemical shift of the signal for the C-19 methyl group (δ_C 15.5), which was further confirmed by the NOESY cross-peaks (Fig. 3) of H₃-19/H₂-6 and of H-7/H₂-9 (δ_H 2.26 and 2.07). The relative configurations of all the asymmetric centers in **7** remained intact, with respect to those of **6**, which was supported by a NOESY experiment. Analogously, the absolute configurations at C-11 and C-12 of **7** were suggested to be the same as those of **4**. The absolute configuration of **7** was tentatively defined as 4*S*,11*R*,12*R*. Therefore, the structure of **7** (the trivial name sarcomililatin D) was proposed as depicted.

Compound **8**, assigned the trivial name sarcomililatinol, was isolated as a colorless oil and exhibited the molecular formula $C_{20}H_{32}O_2$ as determined by its HR-EI-MS peak at m/z 304.2409 $[M]^+$ (Calcd. for $C_{20}H_{32}O_2$, 304.2402), suggestive of 5 degrees of unsaturation, of which one was accounted for by a 14-membered macrocyclic ring, 3 by 2 olefinic bonds, and one by an ether linkage. The intense IR absorption at 3362 cm^{-1} was indicative of the presence of a hydroxyl group. The 1H NMR spectrum (Table 2) showed typical signals for a cembrane nucleus with 2 geminal methyls at δ_H 1.09 (3 H, d, $J = 6.6$ Hz, H₃-17) and 1.07 (3 H, d, $J = 6.6$ Hz, H₃-16), a tertiary methyl at δ_H 1.40 (3 H, s, H₃-20), and 2 vinyl methyls at δ_H 1.71 (3 H, br s, H₃-18) and 1.65 (3 H, br s, H₃-19). The ^{13}C NMR spectrum (Table 2) showed the presence of 20 carbon signals which were classified with the aid of DEPT and HSQC experiments as 5 methyl, 5 methylene, 6 methine (3 sp^2 hybridized and 2 oxygenated), and 4 quaternary (2 sp^2 hybridized and one oxygenated) carbons. The aforementioned data of **8** revealed that it should be a stereoisomer of (+)-11,12-epoxysarcophytol A, which was first isolated from the soft coral *Lobophytum* sp.³⁰. When comparing their ^{13}C NMR spectra, the signals of C-11 and C-12 were shown to be markedly different [δ_C 62.4 and 61.6 for **8**; δ_C 58.4 and 59.8 for (+)-11,12-epoxysarcophytol A, respectively], indicating that the structural difference between them resided in the different configuration of the 11,12-ether linkage. Detailed analysis of its 1H - 1H COSY, HSQC, and HMBC spectra (Fig. 2) allowed the assignment for all proton and carbon resonances of **8**.

The relative configuration of **8** was deduced from interpretation of a NOESY experiment (Fig. 3). The NOESY cross-peaks of H-14 (δ_H 4.86)/H-11 (δ_H 2.68) and Me-20 implied that these protons

were cofacial and were assigned a β -orientation. The geometries of the $\Delta^{1(2)}$, Δ^3 , and Δ^7 double bonds were assigned as *Z*, *E*, and *E*, respectively, on the basis of the carbon chemical shifts of Me-18 (δ_C 17.6) and Me-19 (δ_C 15.3), and this was supported by the key NOESY cross-peaks of H-2 (δ_H 6.02)/H₃-16, H₃-17, and H₃-18; H-3 (δ_H 5.93)/H₂-5 (δ_H 2.20) and H-14; H-7 (δ_H 5.15)/H₂-9 (δ_H 2.24 and 1.09); and H₃-19/H₂-6 (δ_H 2.30 and 2.21). Thus, the relative configuration of **8** was determined as 1*Z*,3*E*,7*E*,11*R**,12*R**,14*S**. However, the absolute configuration of the chiral center at C-14 in **8** was not determined by a modified Mosher's method due to the limited quantity of sample.

In order to determine the absolute configuration of **8**, the TD-DFT ECD calculation method was applied, which has proven to be a powerful and reliable method for the elucidation of the absolute configurations of natural products⁹. As shown in Fig. 6, the ECD spectrum (CH₃CN) of **8** displayed a positive π - π^* Cotton effect at 242 nm. The conformational searches of (11*R*,12*R*,14*S*)-**8** were carried out using the torsional sampling (MCMM) method and OPLS_2005 force field. Conformers above 1% population were re-optimized at the B3LYP/6-311G(d,p) level with IEFPCM (Polarizable Continuum Model using the Integral Equation Formalism variant) solvent model for acetonitrile (Supplementary Information Fig. S1 and Table S1). For the resulting geometries, ECD spectra were obtained by TD-DFT calculations performed with the same functional basis set and solvent model as the energy optimization. Finally, the Boltzmann-averaged ECD spectrum of (11*R*,12*R*,14*S*)-**8** highly matched to the experimental ECD spectrum of **8**, while the enantiomer showed completely opposite curve. Consequently, the absolute configuration of **8** was determined to be 11*R*,12*R*,14*S*.

The known diterpenoids were characterized as (+)-isarsarcophytoxide (**9**)^{19,20} and (+)-isarsarcophine (**10**)³¹ by comparing their observed and reported spectroscopic data. Their HR-MS spectra are also supplied in the Supplementary Information Fig. S72 and Fig. S73, respectively.

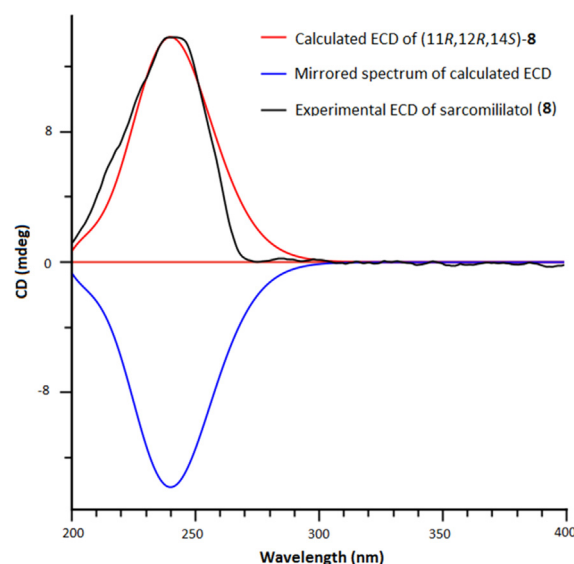
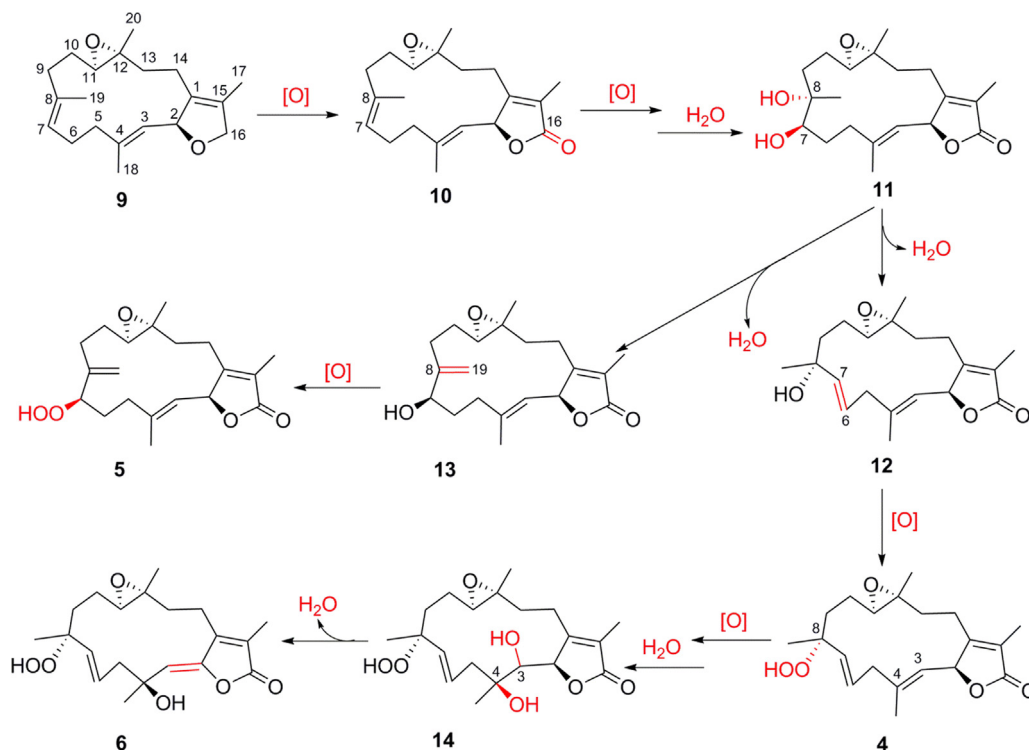


Figure 6 Experimental ECD spectrum of **8** [0.0016 mol/L, CH₃CN, cell length 2 cm] (black) compared with the calculated ECD spectra of **8** (red) and its enantiomer (blue).



Scheme 1 Putative biosynthetic pathways toward the formation of compounds 4–6.

Despite numerous cembrane-type diterpenoids isolated from soft corals of the genus *Sarcophyton*, the investigation of the Et₂O-soluble portion of the acetone extract of the soft coral *S. mililatensis* led to the identification of eight new cembrane diterpenoids (1–8), of which sarcomililatin A–C (4–6) possess a rare hydroperoxy group at C-7 or C-8 in the family of cembrane diterpenoids. To explain the biogenetic origin of compounds 4–6, putative biosynthetic pathways are proposed as shown in Scheme 1. The 3 metabolites can be considered to derive from a common precursor, the co-occurring known cembrane (+)-isarsarcophytoxide (9).

The growth inhibitory potential towards various cancer cell lines of numerous cembrane-type diterpenoids has been documented widely. Accordingly, the cytotoxicities of all the isolates were evaluated *in vitro* against HL-60 and A-549 by using the MTT and SRB methods, respectively. However, all of the tested compound, except for the known compound (+)-isarsarcophytoxide (9), were inactive (IC₅₀ > 10 μmol/L). Compound 9 exhibited strong cytotoxic activities, with IC₅₀ values of 0.78 ± 0.21 and 1.26 ± 0.80 μmol/L against HL-60 and A-549 cells, respectively, comparable to the positive control (adriamycin, IC₅₀ 0.07 μmol/L for HL-60 and 0.01 μmol/L for A-549). In addition, all of the isolated compounds were also subjected to testing *in vitro* for their inhibitory activities against the tumor necrosis factor (TNF)-α-induced nuclear factor (NF)-κB, a transcription factor that plays a critically important role in regulation of cell cycle as well as influencing cell death pathways and has been used as a key target for the treatment of inflammatory diseases and cancer^{32,33}. The results indicated that sarcomililatin A (4) and (+)-isarsarcophytoxide (9) showed moderate inhibitory activities, showing IC₅₀ values of 35.23 ± 12.42 and 22.52 ± 4.44 μmol/L, respectively, compared with the positive control bortezomib (IC₅₀, 0.03 μmol/L), whereas the other compounds were inactive (% inhibition < 50% at 20 μg/mL).

3. Conclusions

A large amount of scientific research has been reported on the specialised metabolite chemistry of soft corals of the genus *Sarcophyton*, whereas related reports on *S. mililatensis* are relatively rare. In the present study, eight new cembrane-type diterpenoids, (+)-(6*R*)-6-hydroxyisarsarcophytoxide (1), (+)-(6*R*)-6-acetoxyisarsarcophytoxide (2), (+)-17-hydroxyisarsarcophytoxide (3), sarcomililatin A–D (4–7), and sarcomililatin (8), were isolated and characterized from the soft coral *S. mililatensis*, along with 2 known ones (9 and 10). The absolute configurations of compounds 4 and 5 were elucidated by ECD spectroscopy, while the absolute configurations of compounds 1 and 8 were established by the modified Mosher's method and TD-DFT ECD calculation, respectively. Among these isolates, compounds 4 and 9 showed inhibitory effects on the TNFα-induced NF-κB activation, while compound 9 also exhibited promising cytotoxicity.

4. Experimental

4.1. General experimental procedures

Optical rotations were measured on a Perkin-Elmer 241MC polarimeter (PerkinElmer, Fremont, CA, USA). UV spectroscopic spectra were recorded in chromatographic grade CH₃OH on a Varian Cary 300 UV–Vis spectrophotometer (Varian, Palo Alto, CA, USA); peak wavelengths are reported in nm. ECD spectra were recorded on a Jasco J-810 spectropolarimeter (JASCO, Japan) at ambient temperature using chromatographic grade CH₃OH and acetonitrile as solvent. IR spectra were recorded on a Nicolet 6700 spectrometer (Thermo Scientific, Waltham, MA, USA); peaks are reported in cm⁻¹. The NMR spectra were measured at 300 K on Bruker DRX 400 and Avance 600 MHz NMR spectrometers (Bruker Biospin AG, Fallanden, Germany). Chemical shifts are

reported in parts per million (δ) in CDCl_3 (δ_{H} reported referred to CHCl_3 at 7.26 ppm; δ_{C} reported referred to CDCl_3 at 77.16 ppm) and coupling constants (J) in Hz; assignments were supported by ^1H - ^1H COSY, HSQC, HMBC, and NOESY experiments. EIMS and HREIMS spectra (70 eV) were recorded on a Finnigan-MAT-95 mass spectrometer (ThermoFisher Scientific, Waltham, USA). ESI-MS and HR-ESI-MS were carried out on a Bruker Daltonics Esquire 3000 plus instrument (Bruker Daltonics K. K., Kanagawa, Japan) and a Waters Q-TOF Ultima mass spectrometer (Waters, MA, USA), respectively. Semi-preparative HPLC was performed on an Agilent-1260 system equipped with a DAD G1315D detector using ODS-HG-5 (250 mm \times 9.4 mm, 5 μm) by eluting with CH_3OH - H_2O or CH_3CN - H_2O system at 3 mL/min. Commercial silica gel (200–300 and 400–500 mesh; Qingdao, China) was used for column chromatography (CC). Precoated SiO_2 plates (HSGF-254; Yantai, China) were used for analytical TLC. Spots were detected on TLC under UV light or by heating after spraying with anisaldehyde H_2SO_4 reagent. Sephadex LH-20 (Amersham Biosciences) was also used for CC. All solvents used for extraction and isolation were of analytical grade.

4.2. Biological material

Specimens of *Sarcophyton mililatensis*, identified by Prof. Hui Huang from South China Sea Institute of Oceanology, Chinese Academy Sciences, were collected along the coast of Weizhou Island (21°0'58" N, 109°6'50" E), Beihai, Guangxi Autonomous Region, China, in May 2007, at a depth of –20 m, and were frozen immediately after collection. A voucher specimen is available for inspection at Shanghai Institute of Materia Medica, SIBS-CAS (No. WZ82).

4.3. Extraction and isolation

The frozen animals (170 g, dry weight) were cut into pieces and ultrasonically extracted with acetone at room temperature (1 L \times 3). The combined acetone extracts were filtered and concentrated *in vacuo*, affording a brown residue, which was suspended in H_2O (4 L) and then partitioned with Et_2O (3 times with 2 L each). The Et_2O -soluble portion (5.0 g) was concentrated in *vacuo*, and then fractionated by silica gel CC (column: 40 cm \times 8 cm) eluting with petroleum ether (PE, 60–90 °C)-acetone (98:2–0:100) to afford nine fractions (A–I), which were combined on the basis of the analysis of TLC.

Fraction D (1.2 g), eluted with PE–acetone (9:1), was initially chromatographed over Sephadex LH-20 (column: 150 cm \times 2 cm), using PE (60–90 °C)- CH_2Cl_2 - CH_3OH (2:1:1) as the mobile phase, to give 5 subfractions (D1–D5). Subfraction D3 (219 mg) was further separated by silica gel CC (column: 20 cm \times 2 cm) eluting with PE (60–90 °C)- CH_2Cl_2 (8:2–3:7), and successively purified by reversed-phase semi-preparative HPLC (column: ODS-HG-5, 250 mm \times 9.4 mm, 5 μm ; mobile phase: CH_3OH - H_2O , 87:13; flow rate: 3 mL/min) to afford compounds **8** (1.5 mg, t_{R} = 14.3 min) and **9** (51.0 mg, t_{R} = 19.8 min).

Fraction E (251 mg), eluted with PE–acetone (8.5:1.5), was initially fractionated by Sephadex LH-20 CC (column: 150 cm \times 2 cm) eluting with PE (60–90 °C)- CH_2Cl_2 - CH_3OH (2:1:1) to give 4 subfractions (E1–E4). Purification of subfraction E2 (79.7 mg) by silica gel CC (column: 20 cm \times 2 cm) eluting with PE (60–90 °C)- Et_2O (7.5:2.5) to afford compound **2** (4.2 mg). Subfraction E3 (56.9 mg) was further chromatographed over silica gel (column: 20 cm \times 2 cm) eluting

with PE (60–90 °C)- Et_2O (8:2) followed by semi-preparative RP-HPLC (CH_3CN - H_2O , 55:45), affording compound **10** (35.7 mg, t_{R} = 22.8 min).

Fraction F (280 mg), eluted with PE–acetone (8:2), was initially chromatographed over silica gel (column: 20 cm \times 3 cm) eluting with CH_2Cl_2 -acetone (10:0–9:1), affording 3 subfractions (F1–F3). Subfraction F2 (70.1 mg) was further separated by Sephadex LH-20 CC (column: 150 cm \times 2 cm) eluting with PE (60–90 °C)- CH_2Cl_2 - CH_3OH (2:1:1), and then purified by semi-preparative RP-HPLC (CH_3CN - H_2O , 60:40) to afford compounds **4** (3.1 mg, t_{R} = 5.8 min) and **5** (6.1 mg, t_{R} = 4.9 min).

Fraction G (1.3 g), eluted with PE–acetone (7:3–6:4), was initially fractionated by Sephadex LH-20 CC (column: 150 cm \times 2 cm) eluting with PE (60–90 °C)- CH_2Cl_2 - CH_3OH (2:1:1) to give 6 subfractions (G1–G6). Subfraction G4 (91.3 mg) was further subjected to silica gel CC (column: 25 cm \times 2 cm) eluting with PE (60–90 °C)-acetone (1:1), yielding compound **7** (2.1 mg) and 3 subfractions (G4-1–G4-3). Purification of subfraction G4-2 (18.5 mg) by semi-preparative RP-HPLC (CH_3CN - H_2O , 55:45) yielded compound **6** (2.0 mg, t_{R} = 7.6 min). Purification of subfraction G6 (170.7 mg) through silica gel CC (column: 20 \times 2 cm) eluting with PE (60–90 °C)- Et_2O (1:1–3:7) followed by semi-preparative RP-HPLC (CH_3CN - H_2O , 50:50) yielded compounds **1** (6.0 mg, t_{R} = 6.7 min) and **3** (3.0 mg, t_{R} = 11.7 min).

4.3.1. (+)-(6R)-6-Hydroxyis sarcophytoxide (1)

Colorless oil; $[\alpha]_{\text{D}}^{25}$ +100 (*c* 0.25, CHCl_3); IR (KBr) ν_{max} 3363, 2961, 2925, 2855, 1755, 1261, 1077, 1033 cm^{-1} ; For ^1H and ^{13}C NMR spectroscopic data, see Table 1; (+)-HR-ESI-MS m/z 341.2096 $[\text{M} + \text{Na}]^+$ (Calcd. for $\text{C}_{20}\text{H}_{30}\text{O}_3\text{Na}$, 341.2087).

4.3.2. (+)-(6R)-6-Acetoxyis sarcophytoxide (2)

Colorless oil; $[\alpha]_{\text{D}}^{25}$ +63 (*c* 0.24, CHCl_3); $[\alpha]_{\text{D}}^{25}$ +53 (*c* 0.5, MeOH); IR (KBr) ν_{max} 2921, 2850, 1732, 1240, 1195, 1131, 1077 cm^{-1} ; For ^1H and ^{13}C NMR spectroscopic data, see Table 1; (+)-HR-ESI-MS m/z 383.2197 $[\text{M} + \text{Na}]^+$ (Calcd. for $\text{C}_{22}\text{H}_{32}\text{O}_4\text{Na}$, 383.2193).

4.3.3. (+)-17-Hydroxyis sarcophytoxide (3)

Colorless oil; $[\alpha]_{\text{D}}^{25}$ +98 (*c* 0.1, CHCl_3); IR (KBr) ν_{max} 3358, 2921, 2851, 1661, 1180, 1131, 1077 cm^{-1} ; For ^1H and ^{13}C NMR spectroscopic data, see Table 1; (+)-HR-ESI-MS m/z 341.2077 $[\text{M} + \text{Na}]^+$ (Calcd. for $\text{C}_{20}\text{H}_{30}\text{O}_3\text{Na}$, 341.2087).

4.3.4. Sarcomilitatin A (4)

Colorless oil; $[\alpha]_{\text{D}}^{25}$ +43 (*c* 0.5, CHCl_3); ECD $\{\text{CH}_3\text{CN}, \lambda[\text{nm}](\Delta\epsilon), c 0.0014 \text{ M}\}$: 249 (–3.1), 221 (+33.4); UV (MeOH) λ_{max} (log ϵ) 246 (2.86), 275 (2.68) nm; IR (KBr) ν_{max} 3356, 2924, 2853, 1751, 1678, 1450, 1180, 1132, 1077 cm^{-1} ; For ^1H and ^{13}C NMR spectroscopic data, see Table 1; (+)-HR-ESI-MS m/z 371.1822 $[\text{M} + \text{Na}]^+$ (Calcd. for $\text{C}_{20}\text{H}_{28}\text{O}_5\text{Na}$, 371.1829).

4.3.5. Sarcomilitatin B (5)

Colorless oil; $[\alpha]_{\text{D}}^{25}$ +34 (*c* 0.1, CHCl_3); $[\alpha]_{\text{D}}^{25}$ +23 (*c* 0.1, MeOH); ECD $\{\text{CH}_3\text{CN}, \lambda[\text{nm}](\Delta\epsilon), c 0.0014 \text{ M}\}$: 249 (–1.5), 223 (+11.3); UV (MeOH) λ_{max} (log ϵ) 247 (2.87), 275 (2.69) nm; IR (KBr) ν_{max} 3358, 2921, 2851, 1659, 1468, 1180, 1132, 1077 cm^{-1} ; For ^1H and ^{13}C NMR spectroscopic data, see Table 2; (+)-HR-ESI-MS m/z 371.1830 $[\text{M} + \text{Na}]^+$ (Calcd. for $\text{C}_{20}\text{H}_{28}\text{O}_5\text{Na}$, 371.1829).

4.3.6. *Sarcomilitatin C* (**6**)

Colorless oil; $[\alpha]_D^{25} +3$ (*c* 0.2, CHCl₃); UV (MeOH) λ_{\max} (log ϵ) 247 (2.72), 288 (2.52), 295 (2.40) nm; IR (KBr) ν_{\max} 3357, 2920, 2850, 1762, 1662, 1463, 1180, 1132, 1077 cm⁻¹; For ¹H and ¹³C NMR spectroscopic data, see Table 2; (–)-HR-ESI-MS *m/z* 363.1813 [M – H][–] (Calcd. for C₂₀H₂₇O₆, 363.1813).

4.3.7. *Sarcomilitatin D* (**7**)

Colorless oil; $[\alpha]_D^{25} +35$ (*c* 0.1, CHCl₃); UV (MeOH) λ_{\max} (log ϵ) 247 (2.73), 286 (2.50), 297 (2.39) nm; IR (KBr) ν_{\max} 3359, 2921, 2851, 1763, 1659, 1632, 1468, 1180, 1132, 1077 cm⁻¹; For ¹H and ¹³C NMR spectroscopic data, see Table 2; (+)-HR-ESI-MS *m/z* 315.1957 [M – H₂O + H]⁺ (Calcd. for C₂₀H₂₇O₃, 315.1955).

4.3.8. *Sarcomilitatol* (**8**)

Colorless oil; $[\alpha]_D^{25} +24$ (*c* 0.1, CHCl₃); ECD { CH₃CN, λ [nm] ($\Delta\epsilon$), *c* 0.0016 M}: 242 (+13.7); UV (MeOH) λ_{\max} (log ϵ) 246 (3.87) nm; IR (KBr) ν_{\max} 3362, 2922, 2852, 1195, 1132, 1077 cm⁻¹; For ¹H and ¹³C NMR spectroscopic data, see Table 2; EI-MS *m/z* 304 [M]⁺ (5), 289 (4), 261 (5), 243 (6), 151 (29), 137 (71), 135 (23), 133 (25), 123 (39), 121 (37), 109 (100), 107 (49); HR-EI-MS *m/z* 304.2409 [M]⁺ (Calcd. for C₂₀H₃₂O₂, 304.2402).

4.3.9. (+)-*Isosarcophytoxide* (**9**)

Colorless oil; $[\alpha]_D^{25} +111$ (*c* 0.6, CHCl₃); lit.: $[\alpha]_D^{24} +160$ (*c* 0.22, CHCl₃)²⁰; (+)-HR-EI-MS *m/z* 302.2240 [M]⁺ (Calcd. for C₂₀H₃₀O₂, 302.2246).

4.3.10. (+)-*Isosarcophine* (**10**)

Colorless oil; $[\alpha]_D^{25} +181$ (*c* 0.2, CHCl₃); lit.: $[\alpha]_D^{24} +170$ (*c* 1.01, CHCl₃)²⁰; (+)-HR-ESI-MS *m/z* 317.2111 [M + H]⁺ (Calcd. for C₂₀H₂₉O₃, 317.2111).

4.4. Preparation of the (*S*)- and (*R*)-MTPA ester derivatives of compound **1**

To 0.92 mg of compound **1** was added 450 μ L of pyridine-*d*₅, and the solution was transferred into an NMR tube. To initiate the reaction, 15 μ L of (*S*)-MTPA-Cl was added with careful shaking and then monitored immediately by ¹H NMR at the following time points: 0, 5, 10, 15, and 20 min. The reaction was found to be complete in 20 min, yielding the mono (*R*)-MTPA ester derivative (**1r**) of **1**.

In an analogous manner, 0.85 mg of compound **1** dissolved in 450 μ L of pyridine-*d*₅ was reacted in a second NMR tube with 15 μ L of (*R*)-MTPA-Cl for 20 min, to afford the mono (*S*)-MTPA ester (**1s**).

4.4.1. (*R*)-MTPA ester (**1r**) of **1**

¹H NMR data of **1r** (400 MHz, pyridine-*d*₅) δ_H 7.570–7.351 (5H, m, Ar-H), 6.147 (1H, ddd, *J* = 10.8, 9.2, 5.6 Hz, H-6), 5.513 (1H, m, H-2), 5.256 (1H, d, *J* = 9.2 Hz, H-7), 5.157 (1H, d, *J* = 9.6 Hz, H-3), 4.581 (1H, dd, *J* = 12.0, 4.0 Hz, H-16a), 4.497 (1H, dd, *J* = 12.0, 3.2 Hz, H-16b), 3.627 (3H, s, OCH₃-MPTA), 2.754 (1H, dd, *J* = 12.4, 5.2 Hz, H-5a), 2.441 (1H, dd, *J* = 11.2, 2.8 Hz, H-11), 2.316 (1H, dd, *J* = 12.4, 10.8 Hz, H-5b), 1.851 (3H, s, H₃-19), 1.608 (3H, s, H₃-17), 1.523 (3H, s, H₃-18), 1.301 (3H, s, H₃-20).

4.4.2. (*S*)-MTPA ester (**1s**) of **1**

¹H NMR data of **1s** (400 MHz, pyridine-*d*₅) δ_H 7.628–7.351 (5H, m, Ar-H), 6.112 (1H, ddd, *J* = 10.8, 9.2, 5.6 Hz, H-6), 5.518 (1H, m, H-2), 5.193 (1H, d, *J* = 9.2 Hz, H-7), 5.120 (1H, d, *J* = 9.6 Hz, H-3), 4.586 (1H, dd, *J* = 12.0, 4.0 Hz, H-16a), 4.502 (1H, dd, *J* = 12.0, 3.2 Hz, H-16b), 3.632 (3H, s, OCH₃-MPTA), 2.801 (1H, dd, *J* = 12.4, 5.2 Hz, H-5a), 2.431 (1H, dd, *J* = 11.2, 2.8 Hz, H-11), 2.444 (1H, dd, *J* = 12.4, 10.8 Hz, H-5b), 1.850 (3H, s, H₃-19), 1.608 (3H, s, H₃-17), 1.532 (3H, s, H₃-18), 1.279 (3H, s, H₃-20).

4.5. Acetylation of compound **1**

Compound **1** (1.2 mg) was dissolved in pyridine (0.5 mL) and Ac₂O (0.5 mL), and the reaction was left to stir at room temperature overnight. MeOH (5 mL) was added to the reaction mixture to remove excess pyridine and Ac₂O *in vacuo*, yielding a brown oil (3.4 mg). The crude product was purified by silica gel CC eluting with PE (60–90 °C)–Et₂O (8:2–7:3) to afford a colorless oil {0.8 mg, $[\alpha]_D^{25} +65$ (*c* 0.09, CHCl₃); $[\alpha]_D^{25} +51$ (*c* 0.09, MeOH)}, which was identical to the natural sample of **2** in all respects.

4.6. ECD calculation of compound **8**

Torsional sampling (MCOMM) conformational searches using OPLS_2005 force field were carried out by means of the conformational search module in the Macro model 9.9.223 software (Schrodinger; <http://www.schrodinger.com/MacroModel>) applying an energy window of 21 kJ/mol, which afforded 74 conformers for **8**. The Boltzmann populations of the conformers were obtained based on the potential energy provided by the OPLS_2005 force field, which afforded 13 conformers for **8** above 1% population for re-optimization. The re-optimization and the following TDDFT calculations of the re-optimized geometries were all performed with Gaussian 09³⁴ at the B3LYP/6–311 G(d,p) level with IEFPCM solvent model for acetonitrile. Frequency analysis was performed as well to confirm that the re-optimized geometries were at the energy minima. Finally, the SpecDis1.62 software³⁵ was used to obtain the Boltzmann-averaged ECD spectrum of the compound and visualize the results as shown (Fig. 6).

4.7. Cytotoxicity bioassays

The cytotoxicities of compounds **1–10** against human promyelocytic leukemia cells (HL-60) and human lung adenocarcinoma cells (A-549) was evaluated by using the MTT and SRB methods, respectively, according to the protocols described in previous literature^{36,37}. The half-maximal inhibition (IC₅₀) was calculated with Graphpad Prism 5.0. IC₅₀ > 10 μ mol/L was considered inactive. Adriamycin was used as the positive control, with IC₅₀ values of 0.07 μ mol/L for the HL-60 cell line and 0.01 μ mol/L for the A-549 cell line, respectively.

4.8. NF- κ B signaling pathway inhibitory activity bioassays

NF- κ B signaling pathway inhibitory activity was evaluated according to the previously reported protocol³⁸. Stable HEK293/NF- κ B cells were plated into 96 well plates at a concentration of approximate 10,000 cells per well. After culturing overnight, compounds were added to the medium at a final concentration

of 10 ng/mL. HEK293/NF- κ B cells were seeded into 96 well cell culture plates (Corning, NY, USA) and allowed to grow for 24 h. The cells were then treated with compounds, followed by stimulation with TNF- α . Four hours later, cell titer blue was added to each well. 2 hours later, the luciferase substrate was added to each well, and the released luciferin signal was detected using an EnVision microplate reader. The IC₅₀ was calculated with Prism 4 software (Graphpad, CA, USA) from the nonlinear curve fitting of the percentage of inhibition (% inhibition) versus the inhibitor concentration [I] by using the Eq. (1):

$$\text{Inhibition (\%)} = 100 / (1 + [IC_{50} / [I]]^k) \quad (1)$$

where k is the Hill coefficient. Bortezomib was used as a positive control with an IC₅₀ value of 0.03 μ mol/L.

Acknowledgments

This work was financially supported by the Natural Science Foundation of China (Nos. 41506187, 81520108028, 21672230 and 81603022), NSFC-Shandong Joint Fund for Marine Science Research Centers (No. U1606403), SCTSM Project (No. 15431901000), the SKLDR/SIMM Projects (SIMM 1705ZZ-01). We thank Prof. Hui Huang from South China Sea Institute of Oceanology, Chinese Academy of Sciences, for the identification of the soft coral material.

Appendix A. Supplementary material

Supplementary data associated with this article can be found in the online version at <https://doi.org/10.1016/j.apsb.2018.06.004>.

References

- Yang B, Zhou XF, Lin XP, Liu J, Peng Y, Yang XW, et al. Cembrane diterpenes chemistry and biological properties. *Curr Org Chem* 2012;**16**:1512–39.
- Gross H, Kehraus S, Nett M, König GM, Beil W, Wright AD. New cytotoxic cembrane based diterpenes from the soft corals *Sarcophyton cherbonnieri* and *Nephthea* sp. *Org Biomol Chem* 2003;**1**:944–9.
- Lin WY, Su JH, Lu Y, Wen ZH, Dai CF, Kuo YH, et al. Cytotoxic and anti-inflammatory cembranoids from the Dongsha Atoll soft coral *Sarcophyton crassocaule*. *Bioorg Med Chem* 2010;**18**:1936–41.
- Lin WY, Lu Y, Su JH, Wen ZH, Dai CF, Kuo YH, et al. Bioactive cembranoids from the dongsha atoll soft coral *Sarcophyton crassocaule*. *Mar Drugs* 2011;**9**:994–1006.
- Saitman A, Sullivan SD, Theodorakis EA. A strategy toward the synthesis of C₁₃-oxidized cembrenolides. *Tetrahedron Lett* 2013;**54**:1612–5.
- Lan J, Liu Z, Yuan H, Peng L, Li WD, Li Y, et al. First total synthesis and absolute configuration of marine cembrane diterpenoid (+)-11,12-epoxysarcophytol A. *Tetrahedron Lett* 2000;**41**:2181–4.
- Li XW, Chen SH, Ye F, Mollo E, Zhu WL, Liu HL, et al. Axiriabilines A–D, uncommon nitrogenous eudesmane-type sesquiterpenes from the Hainan sponge *Axinyssa variabilis*. *Tetrahedron* 2017;**73**:5239–43.
- Xue DQ, Liu HL, Chen SH, Mollo E, Gavagnin M, Li J, et al. 5-Alkylpyrrole-2-carboxaldehyde derivatives from the Chinese sponge *Mycale lissochela* and their PTP1B inhibitory activities. *Chin Chem Lett* 2017;**28**:1190–3.
- Ye F, Zhu ZD, Chen JS, Li J, Gu YC, Zhu WL, et al. Xishacorenes A–C, diterpenes with bicyclo[3.3.1]nonane nucleus from the Xisha soft coral *Sinularia polydactyla*. *Org Lett* 2017;**19**:4183–6.
- Cuong NX, Tuan TA, Kiem PV, Minh CV, Choi EM, Kim YH. New cembranoid diterpenes from the Vietnamese soft coral *Sarcophyton mililatensis* stimulate osteoblastic differentiation in MC3T3-E1 cells. *Chem Pharm Bull* 2008;**56**:988–92.
- Van Minh C, Cuong NX, Tuan TA, Choi EM, Kim YH, Van Kiem P. A new 9,11-secosterol from the Vietnamese sea soft coral, *Sarcophyton mililatensis*, increases the function of osteoblastic MC3T3-E1 cells. *Nat Prod Commun* 2007;**2**:1095–100.
- Khan Z, Bisen PS. Oncoapoptotic signaling and deregulated target genes in cancers: special reference to oral cancer. *Biochim Biophys Acta* 2013;**1836**:123–45.
- Cui CC, Merritt R, Fu LW, Pan Z. Targeting calcium signaling in cancer therapy. *Acta Pharm Sin B* 2017;**7**:3–17.
- Deng J. How to unleash mitochondrial apoptotic blockades to kill cancers?. *Acta Pharm Sin B* 2017;**7**:18–26.
- Wu TC, Geng J, Guo WJ, Gao J, Zhu XX. Asiatic acid inhibits lung cancer cell growth *in vitro* and *in vivo* by destroying mitochondria. *Acta Pharm Sin B* 2017;**7**:65–72.
- Sen R, Baltimore D. Inducibility of Kappa immunoglobulin enhancer-binding protein NF- κ B by a posttranslational mechanism. *Cell* 1986;**47**:921–8.
- Peng S, Hang N, Liu W, Guo WJ, Jiang CH, Yang XL, et al. Andrographolide sulfonate ameliorates lipopolysaccharide-induced acute lung injury in mice by down-regulating MAPK and NF- κ B pathways. *Acta Pharm Sin B* 2016;**6**:205–11.
- Garg A, Aggarwal BB. Nuclear transcription factor- κ B as a target for cancer drug development. *Leukemia* 2002;**16**:1053–68.
- Bowden BF, Coll JC, Heaton A, König G, Bruck MA, Cramer RE, et al. The structures of four isomeric dihydrofuran-containing cembranoid diterpenes from several species of soft coral. *J Nat Prod* 1987;**50**:650–9.
- Wu YC, Hsieh PW, Duh CY, Wang SK, Soong K, Fang LS. Studies on the Formosan soft corals I-Cytotoxic cembrane diterpenes from *Sarcophyton trocheliophorum*. *J Chin Chem Soc* 1992;**39**:355–7.
- Breitmaier E, Voelter W. *Carbon-13 NMR spectroscopy*. 3rd ed. New York: VCH; 1987.
- Tang GH, Sun ZH, Zou YH, Yin S. New cembrane-type diterpenoids from the South China Sea soft coral *Sarcophyton ehrenbergi*. *Molecules* 2016;**21**:E587.
- El Sayed KA, Hamann MT, Waddling CA, Jensen C, Lee SK, Dunstan CA, et al. Structurally novel bioconversion products of the marine natural product sarcophine effectively inhibit JB6 cell transformation. *J Org Chem* 1998;**63**:7449–55.
- Su JH, Ahmed AF, Sung PJ, Chao CH, Kuo YH, Kuo YH, et al. Manaarenolides A–I, diterpenoids from the soft coral *Sinularia manaarensis*. *J Nat Prod* 2006;**69**:1134–9.
- Kobayashi M. Marine terpenes and terpenoids. IV. Isolation of new cembranoid and secocembranoid lactones from the soft coral *Sinularia mayi*. *Chem Pharm Bull* 1988;**36**:488–94.
- Kamel HN, Ferreira D, Garcia-Fernandez LF, Slattery M. Cytotoxic diterpenoids from the hybrid soft coral *Sinularia maxima* \times *Sinularia polydactyla*. *J Nat Prod* 2007;**70**:1223–7.
- Gawronski JK, van Oeveren A, van der Deen H, Leung CW, Feringa BL. Simple circular dichroic method for the determination of absolute configuration of 5-substituted 2(5H)-furanones. *J Org Chem* 1996;**61**:1513–5.
- Bernstein J, Shmeuli U, Zadock E, Kashman Y, Néeman I. Sarcophine, a new epoxy cembranolide from marine origin. *Tetrahedron* 1974;**30**:2817–24.
- Liu KM, Cheng CH, Chen WF, Lu MC, Fang LS, Wen ZH, et al. Trocheliolide A, a hydroperoxycembranoid diterpene from the octocoral *Sarcophyton trocheliophorum*. *Nat Prod Commun* 2015;**11**:63–5.
- Bowden BF, Coll JC, Tapiolas DM. Studies of Australian soft corals. XXXIII. New cembranoid diterpenes from a *Lobophytum* species. *Aust J Chem* 1983;**36**:2289–95.

31. Bowden BF, Coll JC, Hicks W, Kazlauskas R, Mitchell SJ. Studies of Australian soft corals. X. The isolation of epoxyisoneocembrene-A from *Simularia grayi* and isoneocembrene-A from *Sarcophyton ehrenbergi*. *Aust J Chem* 1978;**31**:2707–12.
32. Pikarsky E, Porat RM, Stein I, Abramovitch R, Amit S, Kasem S, et al. NF- κ B functions as a tumour promoter in inflammation-associated cancer. *Nature* 2004;**431**:461–6.
33. Heiss E, Herhaus C, Klimo K, Bartsch H, Gerhäuser C. Nuclear factor κ B is a molecular target for sulforaphane-mediated anti-inflammatory mechanisms. *J Biol Chem* 2001;**276**:32008–15.
34. Frisch MJ, Trucks GW, Schlegel HB, Scuseria GE, Robb MA, Cheeseman JR, et al. *Gaussian 09, Revision B.01*. Wallingford CT: Gaussian, Inc; 2010.
35. Bruhn T, Schaumlöffel A, Hemberger Y, Bringmann G. SpecDis: quantifying the comparison of calculated and experimental electronic circular dichroism spectra. *Chirality* 2013;**25**:243–9.
36. Yu XQ, He WF, Liu DQ, Feng MT, Fang Y, Wang B, et al. A seco-laurane sesquiterpene and related laurane derivatives from the red alga *Laurencia okamurai* Yamada. *Phytochemistry* 2014;**103**:162–70.
37. Yu XQ, Jiang CS, Zhang Y, Sun P, Kurtán T, Mándi A, et al. Compositacins A–K: bioactive chamigrane-type halosesquiterpenoids from the red alga *Laurencia composita* Yamada. *Phytochemistry* 2017;**136**:81–93.
38. Huang RY, Chen WT, Kurtán T, Mándi A, Ding J, Li J, et al. Bioactive isoquinolinequinone alkaloids from the South China Sea nudibranch *Jorunna funebris* and its sponge-prey *Xestospongia* sp. *Future Med Chem* 2016;**8**:17–27.